and characterized.[40] This peptide appears to bind Co^{2+} in a tetrahedral site, with water as the fourth ligand, supporting the plausibility of this sort of structure.

Finally, examination of the sequence data base revealed that three of the metal-binding residues appeared to be completely invariant but the last histidine was occasionally absent with a cysteine appearing in a nearby position. Each of the domains that lack the final histidine is the last one of a tandem array, and the spacings between the histidine and the cysteine are variable. No data have been reported to date concerning whether these domains bind metal ions. To test the hypothesis that a cysteine residue in this region is capable of acting as a ligand, a peptide in which the final histidine in the consensus sequence was replaced by cysteine was synthesized. This peptide (CP-1-H24C) binds metal ions such as Co^{2+} and Zn^{2+}. The absorption spectrum of the Co^{2+} complex is shown in Figure 7. The assignment of the chromophore as $Co(Cys)_3(His)$ is supported by examination of the spectrum of the Co^{2+} complex of a peptide derived from a retroviral nucleocapsid protein that contains an otherwise unrelated metal-binding sequence of the form Cys-X_2-Cys-X_4-His-X_4-Cys, also shown in Figure 7.[41] The spectra are very similar in both the ligand-field and charge-transfer regions. For CP-1-H24C–Co^{2+}, the $^4A_2$ to $^4T_1(P)$ ligand field transition in the visible region is clearly resolved into its three components in a manner similar to that observed for certain synthetic tetrahedral Co^{2+} complexes.[42] Furthermore, this band is red-shifted relative to the parent complex, as would be expected given the positions of thiolate and imidazole in the spectrochemical series.[42,43] The metal ion affinity of CP-1-H24C is comparable to that of the parent peptide, indicating that ligand substitution in this position occurs without a large change in overall metal-binding plus folding energy. In contrast, a His to Cys sequence change resulted in a 10-fold increase in dissociation constant for a retroviral nucleocapsid protein-derived peptide.[44] The availability of zinc finger domains with chemically and spectroscopically differentiated metal-binding sites will be useful for testing models for metal ion binding specificity and for studies of peptides and proteins containing multiple zinc finger domains.

Acknowledgment. Financial support for this work has been provided by the National Institutes of Health (Grant GM-38230), the National Science Foundation (Grant DMB-8850069), and the Chicago Community Trust/Searle Scholars Program. We thank Dr. Joseph Vaughn for assistance in recording some of the NMR spectra. NMR spectrometers were purchased with assistance from grants from the National Institutes of Health (RR-01934, RR-03518) and the National Science Foundation (PCM 83-03176). B.T.A. is the recipient of a fellowship from the Institute for Biophysical Studies of Macromolecular Assemblies supported by the National Science Foundation and V.J.K. is the recipient of a scholarship from the Fulbright Foundation.

Registry No. CP-1, 133551-05-0; [Cys^{24}]-CP-1, 133551-06-1; Co, 7440-48-4; Zn, 7440-66-6.

(40) Merkle, D. L.; Schmidt, M. H.; Berg, J. M. *J. Am. Chem. Soc.*, in press.
(41) Green, L. M.; Berg, J. M. *Proc. Natl. Acad. Sci. U.S.A.* **1989**, *86*, 4047.
(42) Lane, R. W.; Ibers, J. A.; Frankel, R. B.; Papaefthymiou, G. C.; Holm, R. H. *J. Am. Chem. Soc.* **1977**, *99*, 84.
(43) Davis, W. J.; Smith, J. *J. Chem. Soc. A* **1971**, 317.
(44) Green, L. M. Ph.D. Thesis, The Johns Hopkins University, 1990.

Low-Temperature Crystal Structure of Superoxocobalamin Obtained by Solid-State Oxygenation of the B_{12} Derivative Cob(II)alamin†

Erhard Hohenester,‡ Christoph Kratky,*,‡ and Bernhard Kräutler§

Contribution from the Institut für Physikalische Chemie, Universität Graz, A-8010 Graz, Austria, and Laboratorium für Organische Chemie, Eidgenössische Technische Hochschule (ETH), CH-8092 Zürich, Switzerland. *Received September 17, 1990*

Abstract: Exposure of a large (0.3 × 0.3 × 1.0 mm³) "wet" single crystal of cob(II)alamin (B_{12r}, **1**) to gaseous dioxygen (10 atm, 4 °C, 2 days) leads to the formation of the dioxygen adduct $B_{12r}O_2$ (**2**) within the crystal. This solid-state reaction proceeds without affecting the crystalline order, permitting a low-temperature single-crystal structure analysis of $B_{12r}O_2$ (**2**) after rapid cooling of the oxygenated crystal to 96 K. Crystals of $B_{12r}O_2$ (**2**) at 96 K are orthorhombic: space group $P2_12_12_1$, a = 15.749 (13) Å, b = 21.673 (19) Å, c = 25.916 (20) Å, with 4 formula units ($C_{62}H_{88}N_{13}O_{16}PCo$) plus 68 water and 8 acetone molecules per unit cell. The crystallographic refinement (4070 significant observations, 534 parameters) converged at R = 0.095 and R_w = 0.078 and yielded a degree of oxygenation of 0.7. The $B_{12r}O_2$ (**2**) crystal structure is isomorphous to the one of B_{12r} (**1**), but oxygenation leads to structural changes (binding of O_2, upward shift of the cobalt center and of the benzimidazole base) in the cobalamin molecule and to extensive rearrangements in the solvent region. The dioxygen molecule is attached to the metal center in a bent end-on fashion at the β-face of the cobalamin molecule, and it is observed in a single conformation pointing approximately toward C(10) of the corrin ring. All structural evidence is consistent with a formulation of $B_{12r}O_2$ (**2**) as superoxocob(III)alamin. The cobalt-coordinated dioxygen forms hydrogen bonds to two water molecules. The whole solvent region is observed to be fully ordered at 96 K.

Introduction

At low temperature in methanolic solution, the vitamin B_{12} derivative cob(II)alamin (B_{12r}, **1**) is reversibly oxygenated according to Bayston et al.[1] to form what has been termed "superoxocobalamin" ($B_{12r}O_2$, **2**). This species, which is also obtained by the reaction of aquocob(III)alamin (**3**) with superoxide,[2] is assumed to be the first intermediate in the autoxidation

† Dedicated to Prof. A. Eschenmoser on the occasion of his 65th birthday.
‡ Universität Graz.
§ ETH.

(1) Bayston, J. H.; King, N. K.; Looney, F. D.; Winfield, M. E. *J. Am. Chem. Soc.* **1969**, *91*, 2755.
(2) Ellis, J.; Pratt, M. J.; Green, M. *J. Chem. Soc., Chem. Commun.* **1973**, 781.

0002-7863/91/1513-4523$02.50/0

of B_{12r} (1).[1] Under aerobic conditions at room temperature, B_{12r} (1) is rapidly and irreversibly oxidized in solution to a cobalt(III) corrin such as aquocobalamin (3).[3]

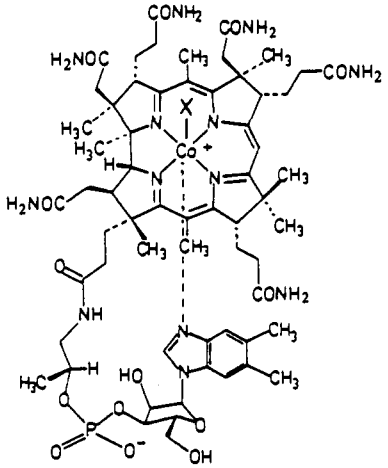

Co–X = Co^{II}: cob(II)alamin (B_{12r}, 1)

Co–X = Co–O_2: superoxocobalamin ($B_{12r}O_2$, 2)

Co–X = Co^{III}–$OH_2^+(Cl^-)$: aquocobalamin chloride (3)

Co–X = Co^{III}–5'-adenosyl: coenzyme B_{12} (4)

Co–X = Co^{III}–CN: cyanocobalamin (vitamin B_{12}, 5)

Reversible oxygenation of B_{12r} (1) at temperatures between −14 and +20 °C was accomplished by Jörin, Schweiger, and Günthard (JSG)[4] in the solid state, using dried crystals of partially reduced aquocobalamin (3), containing 4% B_{12r} (1). By single-crystal EPR of the ^{17}O-enriched dioxygen adduct of vitamin B_{12r} (1), they characterized the pertinent thermodynamic aspects of the solid-state oxygenation reaction, as well as the electronic and the geometric structure and the molecular dynamics of the Co–O_2 fragment. They found the dioxygen ligand to be attached to the metal center in a bent end-on fashion, as observed for biological porphinoid oxygen carriers. One of the motivations for this structure elucidation by EPR techniques[4] was the belief that "evaluation of the structure of $B_{12r}O_2$ from X-ray diffraction analysis appears troublesome because of the difficult growth of pure B_{12r} crystals and their study under high oxygen pressure and low temperature".[4]

Recently, we were able to overcome the first obstacle proposed by JSG and managed to crystallize B_{12r} (1) and determine its crystal structure.[5] This was of interest in particular in connection with questions concerning the biological chemistry of coenzyme B_{12} (4), whose homolysis to B_{12r} (1) and to an adenosyl radical appears to be its biologically most relevant reactivity.[6] Here, we report on the successful solid-state oxygenation of crystals of B_{12r} (1) and on the subsequent low-temperature (96 K) single-crystal structure determination of the so-formed $B_{12r}O_2$ (2).

Superoxocobalamin ($B_{12r}O_2$, 2) has no known biological function, although, according to EPR analyses, it might adventitiously be formed in enzymes containing cobalt(II) corrins in the presence of molecular oxygen.[7] Halpern noted a formal parallel between the reversible cobalt–carbon bond homolysis and the reversible binding of dioxygen, reflected in a similar trend in the dependence of the bond dissociation energies on electronic factors.[8]

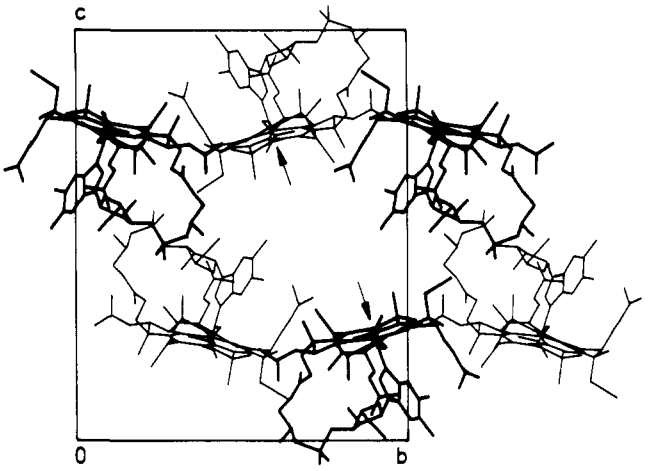

Figure 1. Crystal packing of cob(II)alamin (B_{12r}, 1) molecules in the unit cell viewed along the crystallographic *a* axis. The figure was prepared with coordinates taken from ref 5. Solvent molecules have been omitted for clarity. Arrows mark the positions of the Co(II) centers. The channel runs along one of the crystallographic 2_1 screw axes.

Crystal structure determinations of mononuclear metal complexes with a dioxygen ligand bonded to the metal center are rare: "picket-fence" iron porphyrins have been extensively studied as model systems for heme-containing biological oxygen carriers.[9] Although all these crystal structures contain a disordered dioxygen,[10] a bent end-on coordination of the dioxygen to iron was established, as originally proposed by Pauling for oxyhemoglobin.[11] Several heme-containing proteins in the oxygenated form have been crystallographically studied,[12-14] all of them showing an end-on dioxygen binding mode, with the dioxygen also involved in hydrogen bonds. Accurate geometrical parameters for the metal–dioxygen fragment of the end-on coordinated dioxygen ligand are only available from crystal structure analyses of cobalt–Schiff base complexes,[15-21] the first of which was determined by Rodley and Robinson.[21] Of these crystal structures, only four exhibit a nondisordered, metal-bound dioxygen moiety,[15-18] none of which is involved in hydrogen bonding.

A remarkable feature of the recently determined crystal structure of cob(II)alamin (B_{12r}, 1)[5] is the presence of channels filled with partially disordered water and acetone molecules, as shown in Figure 1. The β-sides of the corrinoid moieties face these at least 6-Å-wide channels, exposing the reactive cobalt(II)

(3) Pratt, M. J. *Inorganic Chemistry of Vitamin B_{12}*; Academic Press: London, 1972; pp 202–204.
(4) (a) Jörin, E.; Schweiger, A.; Günthard, H. H. *J. Am. Chem. Soc.* **1983**, *105*, 4277. (b) Jörin, E. Dissertation No. 7059, ETH Zürich, 1982.
(5) (a) Kräutler, B.; Keller, W.; Kratky, C. *J. Am. Chem. Soc.* **1989**, *111*, 8396. (b) Keller, W. Dissertation, Universität Graz, 1989.
(6) (a) Halpern, J. *Science* **1985**, *227*, 869. (b) Golding, B. T.: Rao, D. N. R. In *Enzyme Mechanisms*; Page, M. I., Williams, A., Eds.; Royal Society of Chemistry: London, 1987; pp 404–428. (c) *B_{12}*; Dolphin, D.; Ed.; Wiley: New York, 1982.
(7) (a) Fraska, V.; Banerjee, R. V.; Dunham, W. R.: Sands, R. H.; Matthews, R. G. *Biochemistry* **1988**, *27*, 8458. (b) Babior, B. M.: Kon, H.; Lecar, H. *Biochemistry* **1969**, *8*, 2662.
(8) Halpern, J. *Pure Appl. Chem.* **1983**, *55*, 1059.
(9) (a) Jones, R. D.; Summerville, D. A.; Basolo, F. *Chem. Rev.* **1979**, *79*, 139 and references therein. (b) Jameson, G. B.; Ibers, J. A. *Comments Inorg. Chem.* **1983**, *2*, 97 and references therein.
(10) (a) Collman, J. P.; Gagne, R. R.; Reed, C. A.; Robinson, W. T.; Rodley, G. A. *Proc. Natl. Acad. Sci. U.S.A.* **1974**, *71*, 1326. (b) Jameson, G. B.; Rodley, G. A.; Robinson, W. T.; Gagne, R. R.; Reed, C. A.; Collman, J. P. *Inorg. Chem.* **1978**, *17*, 850. (c) Jameson, G. B.; Molinaro, F. S.; Ibers, J. A.; Collman, J. P.; Brauman, J. I.; Rose, E.; Suslick, K. S. *J. Am. Chem. Soc.* **1978**, *100*, 6769; **1980**, *102*, 3224.
(11) Pauling, L.; Coryell, C. D. *Proc. Natl. Acad. Sci. U.S.A.* **1936**, *22*, 210.
(12) (a) Philips, S. E. V. *Nature (London)* **1978**, *273*, 247. (b) Philips, S. E. V. *J. Mol. Biol.* **1980**, *142*, 537.
(13) Weber, E.; Steigemann, W.; Jones, T. A.; Huber, R. *J. Mol. Biol.* **1978**, *120*, 327.
(14) Shaanan, B. *Nature (London)* **1982**, *296*, 683.
(15) Avdeef, A.; Schaefer, W. P. *J. Am. Chem. Soc.* **1976**, *98*, 5153.
(16) Gall, R. S.; Rogers, J. F.; Schaefer, W. P.; Christoph, G. C. *J. Am. Chem. Soc.* **1976**, *98*, 5135.
(17) Gall, R. S.; Schaefer, W. P. *Inorg. Chem.* **1976**, *15*, 2758.
(18) Huie, B. T.; Leyden, R. M.; Schaefer, W. P. *Inorg. Chem.* **1979**, *18*, 125.
(19) Schaefer, W. P.; Huie, B. T.: Kurilla, M. G.; Ealick, S. E. *Inorg. Chem.* **1980**, *19*, 340.
(20) Cini, R.; Orioli, P. *J. Chem. Soc., Dalton Trans.* **1983**, 2563.
(21) (a) Rodley, G. A.; Robinson, W. T. *Nature (London)* **1972**, *235*, 438. (b) Rodley, G. A.; Robinson, W. T. *Synth. Inorg. Met.-Org. Chem.* **1973**, *3*, 387.

centers of the B_{12r} molecules to the solvent contained in the channels. This observation invited us to attempt a solid-state synthesis of $B_{12r}O_2$ (**2**) by diffusion of molecular oxygen into B_{12r} (**1**) single crystals, with the ultimate goal of carrying out a crystal structure analysis of the autoxidation intermediate of B_{12r} (**1**). Similar oxygenation reactions have been carried out in the past, both in solution[21b] and in the solid state.[10c] The present experiment stands out by the extreme solution instability of the oxygenation product, which is stabilized by the crystal lattice immobilization. We believe this to be a suitable method for the crystallographic investigation of reaction intermediates whose instability originates from a bimolecular reaction step.

In reporting the crystal structure of coenzyme B_{12} (**4**), Savage et al.[22] noted that both B_{12} crystals and crystals of biological macromolecules show extended regions of (partly disordered) solvent, which makes cobalamin crystals suitable as model systems for the study of hydrogen-bonded water networks.[22c]

Their ability to allow for chemical solid-state reactions by diffusing substrates into intact crystals without affecting the crystalline order is another property that B_{12} crystals share with most crystals of macromolecules. For the latter, this property is routinely exploited for the preparation of isomorphous derivatives[23] or to observe structural changes as a result of the binding of substrates or inhibitors.[24]

Another property common to B_{12} and protein crystals is their high sensitivity toward X-rays, which often prevents the collection of a full intensity data set from *one* crystal specimen.[22a] Low-temperature crystallography of biomolecules[24,25] was considerably enhanced by Hope,[26,27] who pioneered the development of routine techniques to shock-cool macromolecular crystals,[26,28] extending their lifetime in the X-ray beam by several orders of magnitude.[29]

The crystal structure of $B_{12r}O_2$ (**2**) reported here was carried out at 96 K in order to prevent O_2 desorption, to circumvent the problem of radiation damage, and to improve the crystallographic resolution in the solvent region.

Experimental Section

Preparation and Crystallization of B_{12r}. The deoxy compound B_{12r} (**1**) was prepared as described.[5] Crystals grew at room temperature in 3.5-mm glass capillaries during several weeks by vapor diffusion of acetone into an aqueous solution of **1**. Oxygen was strictly excluded, and solvents were purged from dissolved O_2 by freezing and remelting them several times under high vacuum (10^{-5} Torr). Freshly grown crystals of **1** in contact with their mother liquor contain ~20 water molecules and 3 acetone molecules per B_{12r} molecule ("wet" modification).[5b] In contact with air, the crystals lose several solvent molecules to form a "dry" modification.

Preliminary Experiments on "Dry" Crystals. Crystals of **1** were dried by removing them from their mother liquor and placing them on a strip of filter paper at −20 °C for several days. A small "dry" crystal was placed in a 1-mm Mark capillary sealed with a septum, subjected to 2–3 atm of O_2 with the aid of a syringe, and kept at −10 °C for 3 h. Subsequently, crystallographic data were collected at 93 K. The crystal was found to be orthorhombic: space group $P2_12_12_1$, cell constants a = 16.04 (3) Å, b = 20.73 (3) Å, and c = 24.02 (4) Å, V = 7988 (3) Å^3. With respect to "wet" crystals of **1**, a decrease in cell volume of ~1000 Å^3 was observed, corresponding to a loss of about 32 water molecules per unit cell. Intensity data were collected on the diffractometer (see below) to $(\sin\theta)/\lambda$ = 0.364 Å^{-1}, yielding 709 significant ($F_o > 3\sigma(F_o)$) reflections. Several cycles of restrained refinement (101 bond lengths restrained to values observed in the crystal structure of **1**[5]), starting from the coordinates of the crystal structure of ("wet") **1**,[5] yielded a model with R = 0.34 (observation-to-parameter ratio 709/310).

Preparation of $B_{12r}O_2$. The dioxygen adduct of the "wet" modification of **1**, $B_{12r}O_2$ (**2**), was prepared by exposing a freshly grown crystal of **1**, contained in a drop of mother liquor, to 10 atm of O_2 at 4 °C for 2 days in a small autoclave. The transfer of the oxygenated crystal from the autoclave to the diffractometer was carried out at 4 °C and proceeded as quickly as possible in order to minimize O_2 desorption. The crystal was dropped into viscous hydrocarbon oil[27] and was immediately shock-cooled to 96 K in the cold N_2 stream of the low-temperature device of the diffractometer. This mounting procedure took less than 1 min. Since no gas bubbles appeared in the hydrocarbon oil surrounding the crystal, we believe that little decomposition of the sample had occurred during these steps.

Crystallographic Data for $B_{12r}O_2$. Apparent mosaicity (peak width at half peak height for ω scans) ranged from 0.20 to 0.30°. Diffraction data were collected on a modified STOE diffractometer equipped with an Enraf-Nonius cold-stream low-temperature device using graphite-monochromated Mo Kα radiation (λ = 0.71069 Å). Unit cell parameters were obtained by a least-squares refinement against the setting angles of 15 reflections with $2\theta < 7°$. Crystals are orthorhombic, space group $P2_12_12_1$, with 4 formula units ($C_{62}H_{88}N_{13}O_{16}PCo\cdot17H_2O\cdot2(CH_3)_2CO$, formula weight 1361.4 + 416.4) in the unit cell: a = 15.749 (13) Å, b = 21.673 (19) Å, c = 25.916 (20) Å, V = 8845.8 (2.1) Å^3. Since **2** is not stable at ambient conditions, the crystal density could not be determined (d_{calc} = 1.34 g/cm^3). The experimental density for "wet" crystals of **1** is d = 1.34 g/cm^3 (flotation in $CHCl_3$/acetone).

Intensity data were collected at 96 (2) K with an ω step-scan technique with a fixed scan range of $\Delta\omega$ = 1.2° from a crystal of dimensions 0.3 × 0.3 × 1.0 mm^3. The scan speed was variable and ranged from 0.75 to 15°/min depending on the result of a fast prescan with a speed of 15°/min for reflections with $2\theta < 40°$ and 7.5°/min for reflections with $2\theta > 40°$. Stationary-crystal, stationary-counter backgrounds were measured at both ends of the scan, each for one-fourth of the scan time. Three standard reflections from different regions of reciprocal space were periodically monitored (every 100 reflections). The intensities of the standard reflections showed no systematic trends during the 5 days required for data collection, and variations were within the limits of counting statistics.

Net intensities I were calculated as $I = S[C - 2(B_1 + B_2)]$ with C the total integrated peak count, B_1 and B_2 the two background counts, and S the scan rate. Standard deviations $\sigma(I)$ were obtained as $\sigma(I) = S[C + 4(B_1 + B_2)]^{1/2}$. Lorentz and polarization corrections were applied to I and $\sigma(I)$. All reflections for one octant of reciprocal space ($0 \le h \le 17$, $0 \le k \le 23$, $0 \le l \le 28$) with $(\sin\theta)/\lambda \le 0.572$ Å^{-1} were collected, leading to 6790 unique and 4070 significant ($F_o > 3\sigma(F_o)$) reflections.

Refinement of the Structure of $B_{12r}O_2$. Refinement involved minimization of the function $\sum w(|F_o| - |F_c|)^2$ with $w = 1/\sigma^2(F_o)$ with the 4070 significant reflections. Scattering factors were taken from ref 40. Starting from the coordinates of the crystal structure of **1**,[5] several cycles

(22) (a) Savage, H. F. J.; Lindley, P. F.; Finney, J. L.; Timmins, P. A. *Acta Crystallogr., B* **1987**, *43*, 280. (b) Savage, H. F. J. *Biophys. J.* **1986**, *50*, 947. (c) Savage, H. F. J. *Biophys. J.* **1986**, *50*, 967.

(23) McPherson, A. *Preparation and Analysis of Protein Crystals*; Wiley: New York, 1982. (b) Blundell, T. L.; Johnson, L. N. *Protein Crystallography*; Academic Press: London, 1976.

(24) (a) Douzou, P.; Petsko, G. A. *Adv. Protein Chem.* **1984**, *36*, 245.

(25) (a) Low, B. W.; Chen, C. C. H.; Berger, J. E.; Singman, L.; Pletcher, J. F. *Proc. Natl. Acad. Sci. U.S.A.* **1966**, *56*, 1746. (b) Haas, D. J.; Rossmann, M. G. *Acta Crystallogr., B* **1970**, *26*, 998. (c) Thomanek, U. F.; Parak, F.; Mössbauer, R. L.; Formanek, H.; Schwager, P.; Hoppe, W. *Acta Crystallogr., A* **1973**, *29*, 263. (d) Petsko, A. *J. Mol. Biol.* **1975**, *96*, 381. (e) Frauenfelder, H.; Petsko, G. A.; Tsernoglou, D. *Nature (London)* **1979**, *280*, 558. (f) Drew, H. R.; Samson, S.; Dickerson, R. E. *Proc. Natl. Acad. Sci. U.S.A.* **1982**, *79*, 4040. (g) Hartmann, H.; Parak, F.; Steigemann, W.; Petsko, G. A.; Ringe-Ponzi, D.; Frauenfelder, H. *Proc. Natl. Acad. Sci. U.S.A.* **1982**, *79*, 4967.

(26) Hope, H. *Acta Crystallogr., B* **1988**, *44*, 22.

(27) Hope, H. *ACS Symp. Ser.* **1987**, *357*, 257.

(28) Teeter, M. M.; Hope, H. *Ann N.Y. Acad. Sci.* **1986**, *482*, 163.

(29) (a) Hope, H.; Frolow, F.; von Böhlen, K.; Makowski, I.; Kratky, C.; Halfon, Y.; Danz, H.; Webster, P.; Bartels, K. S.; Wittmann, H. G.; Yonath, A. *Acta Crystallogr., B* **1989**, *45*, 190. (b) Dewan, J. C.; Tilton, R. F. *J. Appl. Crystallogr.* **1987**, *20*, 130.

(30) Bieganowski, R.; Kopf, J.; Hinrichs, W.; von Deuten, K. *Acta Crystallogr., A* **1981**, *37*, C235.

(31) (a) Waters, J. M.; Waters, T. N. M. *Proc. Ind. Acad. Sci., Chem. Sci.* **1984**, *93*, 219. (b) Nockolds, C. E.; Ramaseshan, S. *Proc. Natl. Acad. Sci., Chem. Sci.* **1984**, *93*, 197.

(32) Rossi, M.; Glusker, J. P.; Randaccio, L.; Summers, F. M.; Toscano, P. J.; Marzilli, L. G. *J. Am. Chem. Soc.* **1985**, *107*, 1729.

(33) Alcock, N. W.; Dixon, R. M.; Golding, B. T. *J. Chem. Soc., Chem. Commun.* **1985**, 603.

(34) Lenhert, P. G. *Proc. R. Soc. London, Ser. A* **1968**, *303*, 45.

(35) Hinrichs, W.; Klar, G.; Kopf, J.; Wiese, J. *Acta Crystallogr., A* **1984**, *40*, C304.

(36) Stoeckli-Evans, H.; Edmond, E.; Hodgkin, D. C. *J. Chem. Soc., Perkin Trans. 2* **1972**, 605.

(37) (a) Brink-Shoemaker, C.; Cruishank, D. W. J.; Hodgkin, D. C.; Kamper, M. J.; Pilling, D. *Proc. R. Soc. London, Ser. A* **1964**, *278*, 1. (b) Hodgkin, D. C.; Lindsey, J.; Sparks, R. A.; Trueblood, K. N.; White, J. G. *Proc. R. Soc. London, Ser. A* **1962**, *266*, 494.

(38) Hawkinson, S. W.; Coulter, C. L.; Greaves, M. L. *Proc. R. Soc. London, Ser. A* **1970**, *318*, 143.

(39) Kopf, J.; von Deuten, K.; Bieganowski, R.; Friedrich, W. Z. *Naturforsch., C* **1981**, *36*, 506.

(40) *International Tables for Crystallography*; The Kynoch Press: Birmingham, England, 1974; Vol. IV.

of refinement (isotropic atomic displacement parameters (adp's) and unit occupancy for all atoms) with following difference Fourier syntheses yielded the positions of the 2 dioxygen atoms and of 17 water molecules and 2 acetone solvent molecules. An empirical absorption and volume correction[41] (μ = 2.9 cm^{-1}) was applied at this stage. Anisotropic adp's were then assigned to Co, P, and the dioxygen moiety. Hydrogen atoms whose positions are uniquely defined by stereochemistry were included at calculated positions (d(C–H) = 1.08 Å), and only their displacement parameters were refined. No attempts were made to locate methyl or solvent hydrogen atoms.

At this stage, a comparison of the crystal structures of $B_{12r}O_2$ (**2**) and of B_{12r} (**1**) indicated that two atoms of an acetone molecule in the B_{12r} structure (the methyl carbon atom C(401) and the carbonyl oxygen atom O(404)) nearly occupy the same positions as the terminal oxygen atom O(202) and the water molecule O(313) in the $B_{12r}O_2$ structure. Subsequent scrutiny of a difference electron density map showed weak maxima at the positions of the two remaining acetone atoms (C(402) and C(403)), which do not superimpose on any atom in the $B_{12r}O_2$ structure. Therefore, the four atoms of the acetone molecule were included as observed in the 98 K crystal structure of B_{12r} (**1**),[42] without refinement of their atomic coordinates or adp's. Subsequent refinement cycles were based on the assumption that the region around the dioxygen molecule contained either an acetone molecule or the dioxygen moiety plus the two water molecules O(313) and O(314). A single population parameter p was refined for the latter atoms (O(201), O(202), O(313), O(314)), and the atoms of the acetone molecule from the B_{12r} crystal structure (C(401), C(402), C(403) O(404)) were included into structure factor calculations with occupancy $1 - p$. The parameter p refined to a value of 0.69 (2).

Various other models were refined to account for the existence of unoxygenated B_{12r} (**1**) in the crystal investigated. While an occupancy factor of ~0.7 for O_2 was consistently observed, all other models (including one with 30% B_{12r} (**1**) from the 98 K crystal structure substracted as a fixed contribution) gave a significantly worse fit to the experimental data but produced (within the respective standard deviations) the same structural model for the cobalamin molecule.[42b]

Refinement converged at $R = \sum||F_o| - |F_c||/\sum|F_o| = 0.095$ and $R_w = (\sum w(|F_o| - |F_c|)^2/\sum w|F_o|^2)^{1/2} = 0.078$. The final model uses 534 parameters, which amounts to an observation-to-parameter ratio of 7.6/1. The largest peaks in the final difference electron density map were 0.7 (1) e/Å^3, mainly accountable to nonincluded methyl hydrogen atoms. The region around the O_2 molecule did not show features above 0.4 (1) e/Å^3. Computer programs are listed in ref 43.

Results

Preliminary experiments were carried out with dried crystals under conditions resembling the ones chosen by JSG.[4] We found the drying process to be highly irreproducible, resulting in a large decrease in resolution and an increase in mosaic spread relative to freshly grown crystals of B_{12r} (**1**) in contact with their mother liquor ("wet" crystals). Oxygenation of dried crystals and subsequent low-temperature diffraction data collection yielded a limited set of reflection intensities. A difference Fourier synthesis calculated after several cycles of restrained refinement showed a strong electron density peak ~2.0 Å from the cobalt center opposite to the axially coordinated benzimidazole nitrogen atom. Attempts to obtain detailed structural information of the presumed dioxygen adduct of B_{12r} (**1**) were prevented by the poor data quality.

Crystal Structure of $B_{12r}O_2$. Single crystals of B_{12r} (**1**), grown under strict exclusion of oxygen from water/acetone at room temperature, were cooled in an autoclave to 4 °C and exposed to 10 atm of O_2 for 2 days. Since the crystals are highly sensitive to the loss of solvent, they were covered with mother liquor during oxygenation. Subsequently, a crystal was mounted on the diffractometer and quickly cooled to 96 K, as described in the Experimental Section.

The solid-state oxygenation of B_{12r} (**1**) led to single crystals of $B_{12r}O_2$ (**2**), whose crystallographic quality (as judged from the apparent mosaic spread and the resolution) was as good as the one of the parent B_{12r} crystals. X-ray measurements were carried out at 96 K, yielding a very comprehensive set of reflection intensities.

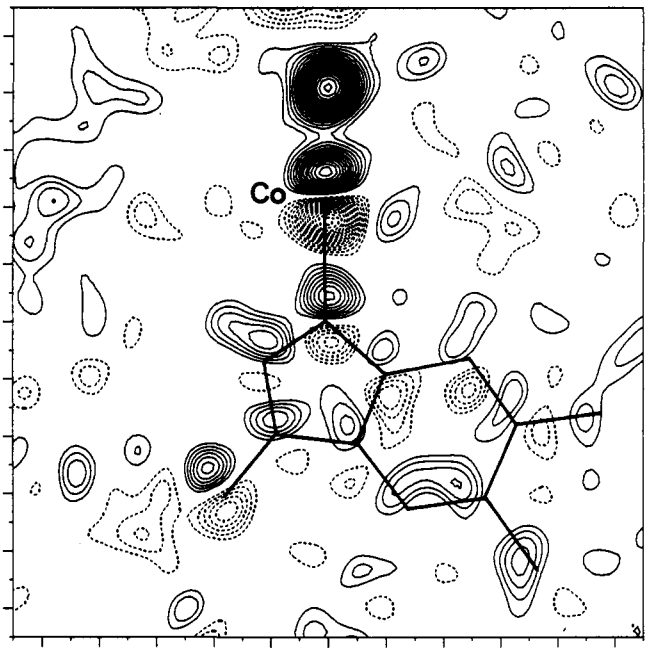

Figure 2. Difference electron density map in a section coincident with the 5,6-dimethylbenzimidazole plane, calculated with coefficients $(|F_o(B_{12r}O_2)| - |F_c(B_{12r})|)\alpha_c(B_{12r})$, where $|F_o(B_{12r}O_2)|$ are the observed structure factor amplitudes of $B_{12r}O_2$ (**2**), $|F_c(B_{12r})|$ are the calculated structure factor amplitudes of B_{12r} (**1**) at 98 K,[42] and $\alpha_c(B_{12r})$ are phases calculated for this model. Positive density is drawn with solid lines and negative with broken lines. Contour lines have been drawn at 0.15 e/Å^3 increment, beginning at 0.25 e/Å^3. The standard deviation of the electron density is about 0.1 e/Å^3.

Comparison of the cell constants of $B_{12r}O_2$ crystals with those of B_{12r} crystals at 98 K[42] (see below) suggested isomorphicity between the two crystal structures. A difference electron density map was calculated with the structural parameters from the 98 K B_{12r} crystal structure; the section coincident with the benzimidazole plane and the cobalt center (Figure 2) indicates (1) the presence of a second axial ligand to the cobalt center, readily identified (from a section perpendicular to the one of Figure 2, not shown) to be a dioxygen ligand; (2) a considerable upward (i.e., toward the dioxygen ligand) shift of the cobalt center; and (3) an upward shift of the whole benzimidazole base.

Refinement converged to a very good fit between observed and calculated structure factors (R = 0.095, R_w = 0.078), compared to other cobalamin crystal structures: (fluoromethyl phosphito–*P*')cobalamin,[30] R = 0.116; cyanocobalamin monocarboxylic acid, R = 0.140[31a] and R = 0.142;[31b] methylcobalamin,[32] R = 0.146; (*R*)-(2,3-dihydroxypropyl)cobalamin,[33] R = 0.085; (*S*)-(2,3-dihydroxypropyl)cobalamin,[33] R = 0.151; 5'-deoxyadenosylcobalamin (coenzyme B_{12}), R = 0.132[34] and R = 0.088,[22a] R = 0.136[22a] and R = 0.085 (neutron);[22a] azidocobalamin,[35] R = 0.20; cyano-13-epicobalamin (neovitamin B_{12}),[36] R = 0.159; cyanocobalamin (vitamin B_{12}, wet),[37a] R = 0.218; vitamin B_{12} 5'-phosphate,[38] R = 0.162; cob(II)alamin (vitamin B_{12r}),[5] R = 0.085; (2-methyladeninyl)cyanocobamide,[39] R = 0.166. The quality of the $B_{12r}O_2$ crystal structure determination is also manifested by the bond lengths (Figure 3), which show good agreement between chemically equivalent bonds and are in agreement with bonding distances expected on the basis of the chemical constitution.[44]

(41) Walker, N.; Stuart, D. *Acta Crystallogr., A* **1983**, *39*, 158.
(42) (a) Hohenester, E.; Keller, W., Kratky, C.; Krăutler, B. Manuscript in preparation. (b) Hohenester, E. Diplomarbeit, Universität Graz, 1990.
(43) (a) Sheldrick, G. M. SHELX-76, a program for crystal structure determination, University of Cambridge, 1976. (b) DIFABS.[41] (c) Johnson, C. K. ORTEP, Report ORNL 5138; Oak Ridge National Laboratory: Oak Ridge, TN, 1976. (d) Motherwell, S. Program PLUTO, University of Cambridge, England.

(44) (a) Rossi, M.; Glusker, J. P. In *Molecular Structure and Dynamics*; Liebmann, J. F., Greenberg, A., Eds.; VCH Publishers: New York, 1988; Vol. 10; p 1. (b) Glusker, J. P. In B_{12}; Dolphin, D., Ed.; Wiley: New York, 1982; Vol. 1, p 23. (c) Pett, V. B.; Liebman, M. N.; Murray-Rust, P.; Prasad, K.; Glusker, J. P. *J. Am. Chem. Soc.* **1987**, *109*, 3207. (d) Kamiya, K.; Kennard, O. *J. Chem. Soc., Perkin Trans. 1* **1982**, 2279.

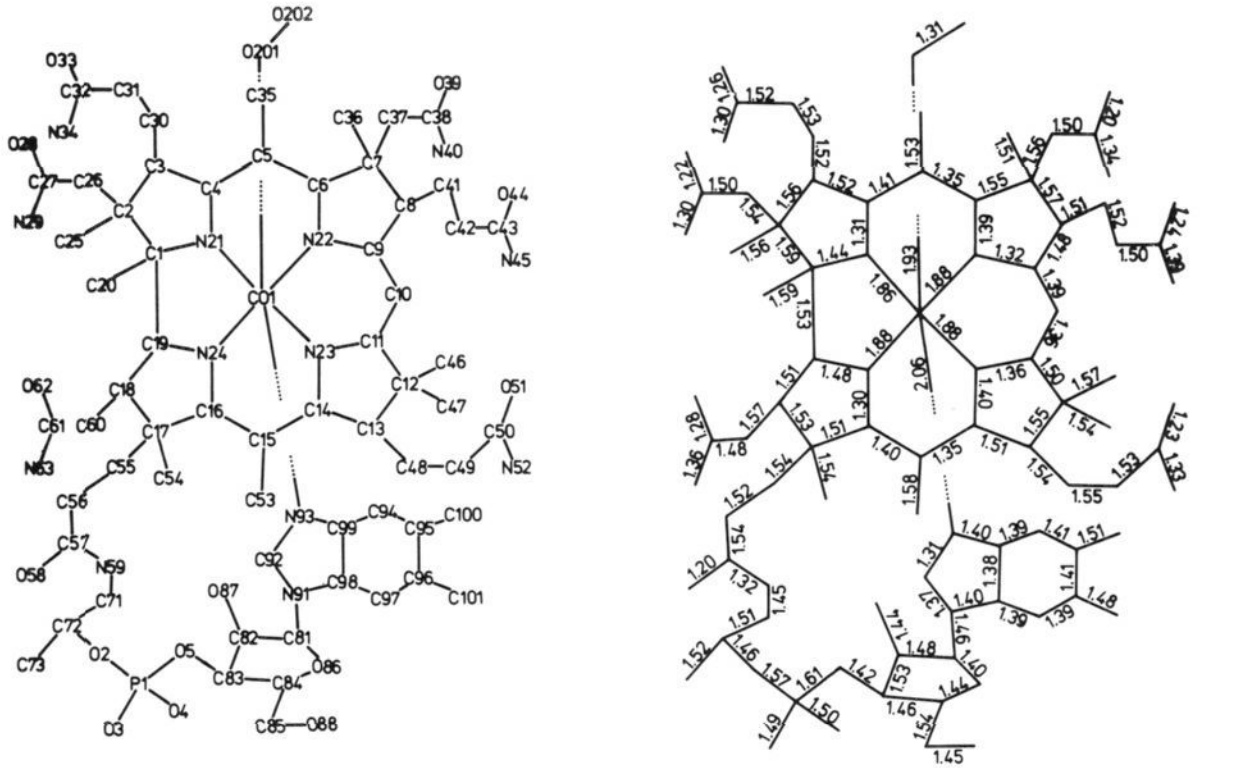

Figure 3. (Left) Numbering scheme for $B_{12r}O_2$ (**2**). (Right) Bond lengths (Å) in the crystal structure of $B_{12r}O_2$ (**2**). Standard deviations: O–O, 0.022 Å; Co–O, 0.015 Å; Co–N and P–O, 0.010 Å; C–X, 0.017···0.025 Å (X = C, N, O).

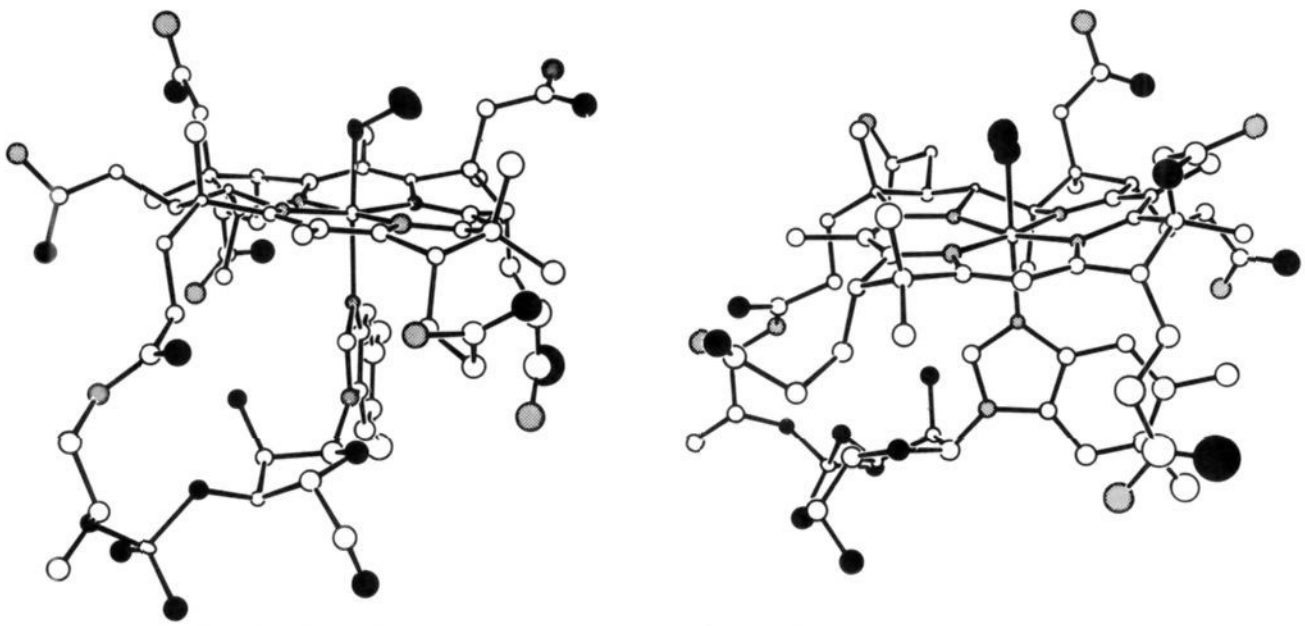

Figure 4. ORTEP drawings of the $B_{12r}O_2$ (**2**) molecule: N, shaded; O, black. Thermal ellipsoids are drawn at the 50% probability level. Hydrogen atoms have been omitted for clarity.

Table I. Bond Angles and Torsion Angles around the Cobalt Center in $B_{12r}O_2$ (**2**)

Co–O(201)–O(202)	120.0 (1.2)	N(22)–Co–N(24)	169.3 (5)	N(21)–Co–N(93)	93.2 (5)
N(21)–Co–N(22)	91.0 (5)	N(21)–Co–O(201)	87.6 (6)	N(22)–Co–N(93)	91.1 (4)
N(21)–Co–N(23)	172.5 (5)	N(22)–Co–O(201)	89.7 (6)	N(23)–Co–N(93)	89.8 (5)
N(21)–Co–N(24)	82.7 (4)	N(23)–Co–O(201)	89.7 (6)	N(24)–Co–N(93)	97.8 (5)
N(22)–Co–N(23)	95.9 (5)	N(24)–Co–O(201)	84.8 (5)	O(201)–Co–N(93)	177.4 (5)
N(22)–Co–O(201)–O(202)	−55 (1)	N(21)–Co–N(93)–C(92)	−131 (1)	N(23)–Co–N(93)–C(92)	42 (1)
N(23)–Co–O(201)–O(202)	41 (1)	N(22)–Co–N(93)–C(92)	138 (1)	N(24)–Co–N(93)–C(92)	−48 (1)
[Co–O(201)]–[4N–plane]	90.0 (5)				

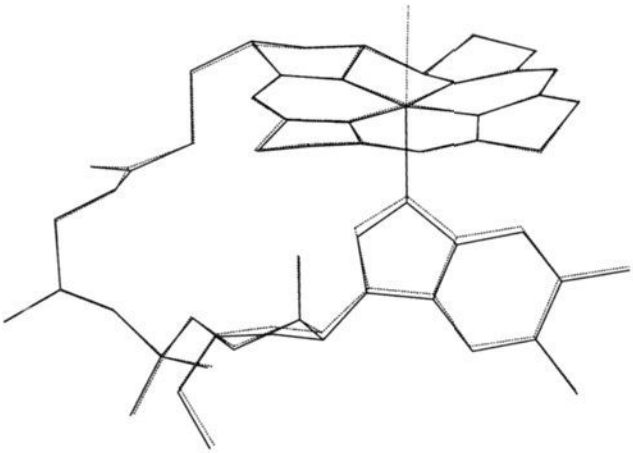

Figure 5. Superposition of the B_{12r} (**1**) (solid line) and the $B_{12r}O_2$ (**2**) (broken line) molecules. Only the corrin macrocycle (plus the cobalt center) and the nucleotide loop are shown. The C and N atoms of the corrin moiety were matched by least squares (rms distance of equivalent corrin atoms 0.06 Å).

Likewise, the ORTEP[43c] drawings of the $B_{12r}O_2$ molecule displayed in Figure 4 show a uniform distribution of (isotropic) adp's, indicative of the absence of severe systematic errors in the reflection data.

Atomic coordinates and adp's of the $B_{12r}O_2$ crystal structure have been deposited as supplementary material. Table I lists selected bond angles and torsion angles.

Oxygenation occurs with extensive rearrangement in the solvent region. Of the 15 water and 3 acetone molecules per asymmetric unit of the B_{12r} crystal structure, only 10 water and 2 acetone sites were observed in the $B_{12r}O_2$ crystal structure (within 0.5 Å). Seven additional water molecules of the $B_{12r}O_2$ crystal structure do not superimpose on any solvent site of the B_{12r} structure. The one acetone molecule lost upon oxygenation from a position ~3.4 Å above the corrin ring plane in the B_{12r} crystal structure is displaced by the dioxygen in $B_{12r}O_2$.

The $B_{12r}O_2$ crystal structure is isomorphous to the parent B_{12r} crystal structure. The only significant difference is a shrinkage of the *c* axis by about 0.43 (5) Å, which amounts to a 100 Å^3 (1%) shrinkage of the cell volume upon oxygenation. A normal probability plot (NPP) analysis[45] of its fractional *z* coordinates reveals that the corrin fragment retains its structural identity within experimental error but is shifted by ~0.02 Å (Figure S1, supplementary material).

The $B_{12r}O_2$ crystal investigated contained about 30% unoxygenated B_{12r} (1). The "ghost" of an acetone molecule located above the (unoccupied) upper (β) coordination site in the B_{12r} crystal structure was observed in a difference electron density map, leading to a model consisting of a superposition of 70% $B_{12r}O_2$ (**2**) with 30% B_{12r} (**1**). This model yielded a moderate improvement in the fit to the experimental *F* values (i.e., a decrease in R_w from 0.081 to 0.078 upon inclusion of one additional parameter), and it had a beneficial effect on the adp's of the dioxygen moiety: A model with unit occupancy for O_2 resulted in large adp's for both dioxygen atoms, violating Hirshfeld's rigid-bond postulate[46] for the axial Co–O bond. The superposition model involving 70% $B_{12r}O_2$ (**2**) and 30% B_{12r} (**1**) (see the Experimental Section) yielded reasonable adp's for the dioxygen, which were in agreement with the rigid-bond postulate (librational component along the Co–O bond: (1) for $p = 1.0$, Co(1) 0.014 (1) Å^2, O(201) 0.082 (11) Å^2; (2) for $p = 0.7$, Co(1) 0.015 (1) Å^2, O(201) 0.022 (8) Å^2).

The crystal structure of $B_{12r}O_2$ shows a bent end-on coordinated dioxygen molecule, which does not suffer from conformational disorder. The geometrical parameters of the metal coordination

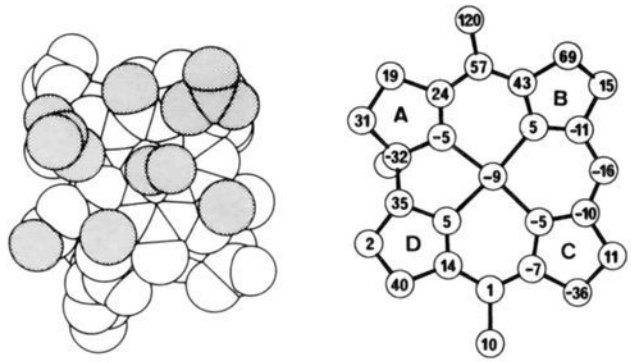

Figure 6. (Left) Space-filling representation of the $B_{12r}O_2$ (**2**) molecule viewed along O(201)–Co(1). Atoms more than 1 Å above the 4N-plane are shaded. (Right) Deviations (Å × 100) of corrin atoms from the 4N-plane in the $B_{12r}O_2$ (**2**) molecule. Standard deviations are ~0.005 Å for cobalt and ~0.02 Å for carbon and nitrogen.

of O_2 are given in Figure 3 and in Table I: O_2 is inclined with respect to the corrin ring plane, and it points toward the meso carbon atom C(10) between the pyrrolic rings B and C. The dihedral angle between the Co–O–O plane and a least-squares plane through the atoms of the benzimidazole base is 97 (2)°.

The molecular geometries of the corrin portion of B_{12r} and $B_{12r}O_2$ are very similar, as is evident from the superposition of the two molecules shown in Figure 5. The only crystallographically significant differences are as follows: The oxygenated species shows the cobalt center 0.09 (1) Å below the N_4 plane, which amounts to an upward shift of the metal center by 0.05 Å with respect to B_{12r} (**1**). The axial Co–N bond to the benzimidazole nitrogen atom (2.06 (1) Å in $B_{12r}O_2$ (**2**)) is shorter by 0.09 Å than in B_{12r} (**1**) (2.15 (1) Å), resulting in an upward shift of the whole base with respect to the corrin ring plane. This is accommodated for by a conformation change in the ribose part of the nucleotide loop (the puckering amplitude[47] of the ribose ring is 0.34 (1) Å in $B_{12r}O_2$ (**2**) and 0.43 (1) Å in B_{12r} (**1**)).

Discussion

A frequently discussed mechanism for the autoxidation of B_{12r} (**1**) involves a μ-peroxo complex as reaction intermediate. Experimental support for such a mechanism exists for cobalt(II) cobaloximes,[48] which are often used as B_{12} models. It is also known that the kinetics of the autoxidation reaction shows second-order dependence on the B_{12r} concentration at 0 °C in aqueous solution.[49]

The fact that, in the solid state, the oxygenation reaction does not proceed beyond the formation of the dioxygen adduct (the proposed first autoxidation intermediate) is consistent with this mechanistic picture. Packing of B_{12r} molecules into a crystal results in an immobilization, which would inhibit the formation of the dimeric μ-peroxo intermediate. A similar reason—steric prevention of dimer formation—may account for the insensitivity of protein-bound B_{12r} toward autoxidation in the presence of air.[7,49,50]

In the crystal of $B_{12r}O_2$, the dioxygen moiety is attached to the cobalt center in a bent end-on fashion, inclined toward the meso carbon C(10). The conformation obtained by JSG[4] from an analysis of the EPR spectra of dried $B_{12r}O_2$ crystals below 110 K is very similar, which is remarkable in view of the assumptions (unchecked at the time) underlying the EPR analysis (isomorphicity between the crystals of **1**, **2**, **3**, and **5**).

JSG ascribe the perpendicular conformation of the dioxygen with respect to the plane of the axial base primarily to electronic effects. Since both, perpendicular[21,51] and parallel arrange-

(45) (a) Abrahams, S. C.; Keve, E. T. *Acta Crystallogr., A* **1971**, *27*, 157. (b) Hamilton, W. C. *Acta Crystallogr., A* **1972**, *28*, 215.
(46) Hirshfeld, F. L. *Acta Crystallogr., A* **1976**, *32*, 239.
(47) Dunitz, J. D. *X-Ray Analysis and the Structure of Organic Molecules*; Cornell University Press: Ithaca, NY, 1979; pp 425–431.
(48) Schrauzer, G. N.; Lee, L. P. *J. Am. Chem. Soc.* **1970**, *92*, 1551.
(49) Abel, E. W.; Pratt, J. M.; Whelan, R.; Wilkinson, P. J. *S. Afr. J. Chem.* **1977**, *30*, 1.
(50) Toraya, T.; Ushio, K.; Fukui, S.; Hogenkamp, H. P. C. *J. Biol. Chem.* **1977**, *252*, 963.
(51) Calligaris, M.; Nardin, G.; Randaccio, L.; Tauzher, G. *Inorg. Nucl. Chem. Lett.* **1973**, *9*, 419.

ments,[15-20] have been reported for crystal structures of dioxygen adducts of Schiff base complexes, electronic effects of the axial base on the Co–O–O conformation through the equatorial plane are likely to be of secondary importance. A space-filling representation of the $B_{12r}O_2$ molecule from the present crystal structure analysis (shown in Figure 6) suggests that there are essentially two sterically favoured O_2 conformations. The one of these actually observed places the dioxygen moiety above the slightly downward folded segment of the corrin ring.

All features of its crystal structure are consistent with a description of $B_{12r}O_2$ as superoxocob(III)alamin. The O–O bond length of 1.32 (2) Å agrees with values observed for the most accurate cobalt(III) superoxo complexes,[9a,15-18,52] and the contraction of the axial Co–N bond from 2.15 (1) Å (B_{12r}, **1**) to 2.06 (1) Å ($B_{12r}O_2$, **2**) indicates a decrease of electron density at the cobalt center, compatible with its formulation as Co(III). So far, the value of 2.06 (1) Å for the axial Co–N bond length in **2** can only be compared to the axial Co–N bond lengths found in cyanocob(III)yrinates, which range from 1.97 to 2.06 Å,[31,36,37] as a crystal structure of a cob(III) alamin with an upper oxygen ligand—such as aquocobalamin (**3**)—is not yet available. A description of $B_{12r}O_2$ (**2**) as superoxocobalamin is also supported by the detailed interpretation of the EPR data of $B_{12r}O_2$ (**2**) given by JSG.

Degree of Oxygenation. According to the thermodynamic parameters (ΔH_o = −6 kcal/mol, ΔS_o = −20 cal/mol·K)[4] and kinetic observations (equilibration after several hours),[4b] the conditions chosen by us (p = 10 atm, T = 277 K, 2 days) should lead to a degree of oxygenation in excess of 95%, provided the thermodynamic and kinetic properties are the same for "dry" aquocobalamin crystals containing 4% B_{12r} as for "wet" B_{12r} crystals. Exposure of a ("wet") crystal to the above conditions led to only 70% oxygenation, as judged from the crystallographic results. Possible reasons for the lower than expected degree of oxygenation are (1) different thermodynamic parameters, (2) a slower rate of oxygenation, and (3) O_2 desorption during transfer of the oxygenated crystal from the autoclave to the cryostat of the diffractometer.

While the present experiment yields no evidence pertaining to a possible difference in the thermodynamic parameters of the oxygenation reaction, a slowdown in the reaction rate (relative to "dry" B_{12r} crystals) due to the additional out-diffusion of acetone is very probable. A loss of O_2 during crystal manipulation is unlikely in view of the observation of an acetone "ghost".

The $B_{12r}O_2$ crystal contains about 30% unoxygenated B_{12r}, and our model refined against intensity data collected from this crystal should therefore display features of a superposition of two similar but not identical structures. While, as shown above, this is the case for the region of the upper (β) axial coordination site (observation of the "ghost" of an acetone molecule from the B_{12r} crystal structure), we curiously see no such effects for the nucleotide loop. In this region, where the two structures differ significantly (up to 0.2 Å; see Figure 5), one would expect to observe positive or negative difference electron density (in a final ΔF map) and/or a significant increase in the corresponding adp's. Moreover, the superposition of two structures could lead to chemically unreasonable geometrical parameters. Neither of these effects are observed: the difference electron density map around the benzimidazole base is essentially featureless (Figure S2, supplementary material), and the adp's for the nucleotide loop do not show any dependence on the shift of the corresponding atom upon oxygenation. Finally, the bond lengths of the nucleotide are within experimental error the same as the ones observed in the crystal structure of 5,6-dimethylbenzimidazole[53] and of B_{12r} (**1**) at 98 K.[42]

Cooling to 96 K leads to almost complete ordering of the solvent molecules. Previous B_{12} structure determinations[5,22a,30-39] were plagued by difficulties in modeling the electron density of extended regions of disordered solvent molecules: Savage et al.[22] had to postulate several overlapping and mutually exclusive solvent networks in their analysis of the coenzyme B_{12} crystal structure. A similar situation exists in the (as yet unpublished[5b]) room-temperature B_{12r} crystal structure. We believe structure determination at cryogenic temperature to be superior to collecting diffraction data at temperatures above 0 °C: Compared to Savage's analysis,[22] our data can be fitted at a comparable level of agreement with a fraction of their number of parameters. Apart from the ordering of solvent regions, cryogenic temperatures lead to a decrease of thermal libration, which obviates the refinement of anisotropic adp's for the majority of atoms.

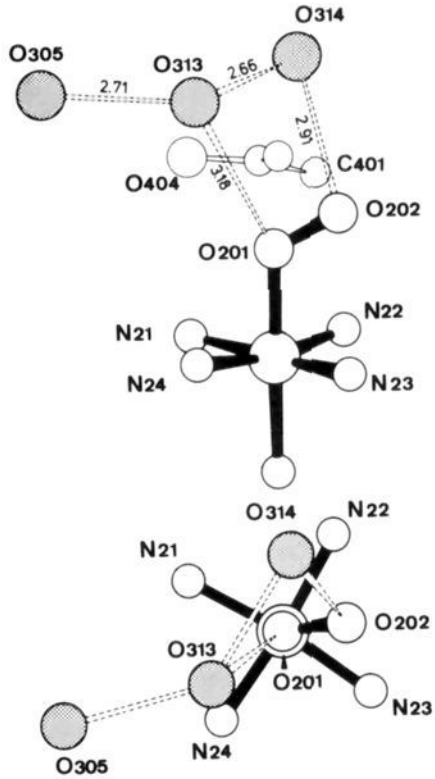

Figure 7. Hydrogen bonding to the dioxygen ligand in the crystal structure of $B_{12r}O_2$ (**2**). Solvent water molecules are shaded. The position of an acetone molecule observed in the crystal structure of B_{12r} (**1**) at 98 K[42] is also shown (in the B_{12r} crystal structure, the acetone carbonyl oxygen atom O(404) is hydrogen bonded to a water molecule observed at the O(305) site). Standard deviations of distances shown in this figure range from 0.05 to 0.08 Å. Angles: O(201)–O(313)–O(314), 70(2)°; O(313)–O(314)–O(202), 74(2)°; O(314)–O(202)–O(201); 100(2)°; O(202)–O(201)–O(313), 86(2)°; O(313)–O(201)–O(202)–O(314), 41(2)°.

There are two hydrogen bonds connecting the metal-coordinated dioxygen to the water network. Their existence is indicated by the contacts between O(313) and O(201) (d = 3.18 (7) Å) and between O(314) and O(202) (d = 2.91 (5) Å). The detailed geometry of these two hydrogen bonds is contained in Figure 7.

So far, only few hydrogen bonds to an end-on coordinated dioxygen have been crystallographically observed.[12-14,54] There exists much evidence for a biological relevance of hydrogen bonding to metal-coordinated dioxygen: A hydrogen bond of the O_2 to the distal histidine has been proposed to account for the increased oxygen affinity of haemoglobin and myoglobin relative to unprotected iron(II) porphyrinato systems.[55] The presence of such a hydrogen bond has been postulated on the basis of the results of infrared,[56] resonance Raman,[57] kinetic,[58] and EPR[59]

(52) Vaska, L. *Acc. Chem. Res.* **1976**, *9*, 175.
(53) Young, J. L.; Scheidt, W. R. *Acta Crystallogr., C* **1986**, *42*, 1652.
(54) Brown, L. D.; Raymond, K. N. *Inorg. Chem.* **1975**, *14*, 2595.
(55) (a) Drago, R. S.; Cannady, J. P.; Leslie, K. A. *J. Am. Chem. Soc.* **1980**, *102*, 6014. (b) Drago, R. S. *Acc. Chem. Res.* **1980**, *13*, 353.
(56) (a) Barlow, C. H.; Maxwell, J. C.; Wallace, W. J.; Caughey, W. S. *Biochem. Biophys. Res. Commun.* **1973**, *55*, 91. (b) Maxwell, J. C.; Volpe, J. A.; Barlow, C. H.; Caughey, W. S. *Biochem. Biophys. Res. Commun.* **1974**, *58*, 166.

studies and was directly observed in the neutron crystal structure analysis of oxymyoglobin.[60] Furthermore, the influence of hydrogen bonding to the dioxygen on the O_2 affinity of model systems, such as cobalt Schiff base complexes[55] and "picket-fence" iron porphyrins[61] has been clearly established.

In the crystal structure of $B_{12r}O_2$ (2), both O_α and O_β are involved in hydrogen bonding interactions. The observation of these two hydrogen bonds is also consistent with the description of $B_{12r}O_2$ (2) as superoxocobalamin, which predicts a considerable charge transfer onto the dioxygen ligand.

Acknowledgment. We thank Dr. Arthur Schweiger, ETH Zürich, for helpful discussions. Financial support from the Swiss and Austrian National Science Foundations is acknowledged.

Supplementary Material Available: X-ray structural data for superoxocobalamin ($B_{12r}O_2$, 2), including tables of atomic coordinates, anisotropic and isotropic atomic displacement parameters, bond lengths, bond angles, torsion angles, and hydrogen-bonding distances and figures showing a normal probability plot of the differences in the z coordinates of 2 and 1 for the atoms of the corrin ring and a section through the benzimidazole plane of the final difference Fourier synthesis (11 pages). Ordering information is given on any current masterhead page.

(57) (a) Tsubaki, M.; Yu, N. T. *Proc. Natl. Acad. Sci.* U.S.A. **1981**, *78*, 3581. (b) Kitagawa, T.; Ondrias, M. R.; Rousseau, D. L.; Ikeda-Saito, M.; Yonetani, T. *Nature (London)* **1982**, *298*, 869. (c) Bajdor, K.; Kincaid, J. R.; Nakamoto, K. *J. Am. Chem. Soc.* **1984**, *106*, 7741.
(58) Mims, M. P.; Porras, A. G.; Olson, J. S.; Noble, R. W.; Peterson, J. A. *J. Biol. Chem.* **1983**, *258*, 14219.
(59) (a) Yonetani, T.; Yamamoto, H.; Iizuka, T. *J. Mol. Biol.* **1974**, *249*, 2168. (b) Ikeda-Saito, M.; Iizuka, T.; Yamamoto, H.; Kayne, F. J.; Yonetani, T. *J. Biol. Chem.* **1977**, 252, 4882. (c) Walker, F. A.; Bowen, J. *J. Am. Chem. Soc.* **1985**, *107*, 7632.
(60) Philips, S. E. V.; Schoenborn, B. P. *Nature (London)* **1981**, *292*, 81.
(61) Jameson, G. B.; Drago, R. S. *J. Am. Chem. Soc.* **1985**, *107*, 3017.

Keto-Enol Tautomerization in Metal-Acyl Complexes: The Enolization Properties of Bimetallic μ-Malonyl Compounds

Joseph M. O'Connor,*[†,1a] Roger Uhrhammer,[1a] Arnold L. Rheingold,*[1b] and Dean M. Roddick*[1c]

Contribution from the Departments of Chemistry, University of California at San Diego, La Jolla, California 92093-0506, University of Delaware, Newark, Delaware 19716, and University of Wyoming, Laramie, Wyoming 82071. *Received October 22, 1990*

Abstract: In THF solution, $(\eta^5\text{-}C_5Me_5)(NO)(PPh_3)Re[\mu\text{-}(COCH_2CO)\text{-}C^1,O^3\text{:}C^3]Re(CO)_4$ (2-Re) exists in equilibrium with its enol tautomer $(\eta^5\text{-}C_5Me_5)(NO)(PPh_3)Re\{\mu\text{-}[COCH{=}C(OH)]\text{-}C^1,O^3\text{:}C^3\}Re(CO)_4$ (2-Re-OH), with $K_{eq}^{23°C}$ = [2-Re-OH]/[2-Re] = 0.66. The enol form of the manganese analogue $(\eta^5\text{-}C_5Me_5)(NO)(PPh_3)Re[\mu\text{-}(COCH_2CO)\text{-}C^1,O^3\text{:}C^3]Mn(CO)_4$ (2-Mn) is not observed by NMR spectroscopy in THF. When the enolate anion, $(\eta^5\text{-}C_5Me_5)(NO)(PPh_3)Re\{\mu\text{-}[COCH{=}C(OLi)\text{-}C^1,O^3\text{:}C^3]Mn(CO)_4$ (2-Mn-OLi) is protonated at low temperature, 2-Mn-OH is generated and completely converted to 2-Mn at room temperature, $K_{eq}^{23°C}$ = [2-Mn-OH]/[2-Mn] <0.02. Both 2-Re and 2-Mn undergo stereoselective exchange of the malonyl ligand hydrogens with deuterium in D_2O. The equilibrium acidity of 2-Re was determined by measuring the ratio of 2-Re to 2-Re-OLi when THF solutions of 2-Re-OLi were treated with 1 equiv of methyl acetoacetate (complete conversion to 2-Re), dimethyl malonate (59% conversion to 2-Re), or methanol (no conversion to 2-Re). The thermodynamic acidity of 2-Re is therefore similar to that of dimethyl malonate in THF. When THF solutions of 2-Re-OLi were treated with 2-Mn, the microscopic acidity of 2-Re was determined to be greater than that of 2-Mn with K = [2-Re-OLi][2-Mn]/[2-Re][2-Mn-OLi] = 80 at -80 °C. The trimethylsilyl enol ethers $(\eta^5\text{-}C_5Me_5)(NO)(PPh_3)Re\{\mu\text{-}[COCH{=}C(OSi(CH_3)_3)]\text{-}C^1,O^3\text{:}C^3\}M(CO)_4$ (2-Re-OSi, M = Re and 2-Mn-OSi, M = Mn) were prepared and structurally characterized as models for 2-Re-OH and 2-Mn-OH. A comparison of the solid-state structures for 2-Re, 2-Mn, 2-Re-OSi, and 2-Mn-OSi indicates that the metallafuran rings in 2-Mn-OH and 2-Re-OH are not significantly aromatic in character. 2-Mn-OSi undergoes hydrolysis in wet THF-d_8 17 times faster than does 2-Re-OSi. The first nonchelating μ-malonyl complex $(\eta^5\text{-}C_5Me_5)(NO)(PPh_3)Re[\mu\text{-}(COCH_2CO)\text{-}C^1\text{:}C^3]Re(CO)_4(PMe_3)$ (5) was prepared by lithium ion abstraction from $\{(\eta^5\text{-}C_5Me_5)(NO)(PPh_3)Re[\mu\text{-}(COCH_2CO)\text{-}C^1\text{:}C^3]Re(CO)_4(PMe_3)\}\cdot Li^+OSO_2CF_3^-$ (4) with 211-kryptofix. In THF 5 exists in equilibrium with its enol tautomer, $(\eta^5\text{-}C_5Me_5)(NO)(PPh_3)Re\{\mu\text{-}[COCH{=}C(OH)]\text{-}C^1\text{:}C^3\}Re(CO)_4(PMe_3)$ (5-OH), with K_{eq} = [5-OH]/[5] = 0.65. The X-ray structures of 5 and 5-OH were determined.

Introduction

The properties and reactivity of organic carbonyl compounds are strongly influenced by keto-enol tautomerization.[2] For example, enols are key intermediates in aldol condensations, electrophilic substitution in carbonyl compounds, and a number of important molecular rearrangements.[3] It is therefore quite striking that, until the work reported here, the enol form of metal-acyl complexes had yet to be observed under conditions of equilibrium with the keto tautomer.[4,5] It is to be expected that access to enolization phenomena in metal acyls will further expand the reactivity manifold available to this important compound class. In organic systems the enol form is often observable and may even be the favored tautomer when the enol is conjugated with an unsaturated substitutent. Furthermore, 1,3-dicarbonyls provide

† Address correspondence to this author at Department of Chemistry, University of Nevada, Reno, NV 89557.

(1) (a) University of California, San Diego. (b) University of Delaware. (c) University of Wyoming.
(2) (a) Forsen, S.; Nilsson, M. In *The Chemistry of the Carbonyl Group, II*; Patai, S., Ed.; Wiley Interscience: New York, 1970. (b) Zimmerman, H. E. *Acc. Chem. Res.* **1987**, *20*, 263 and references therein. (c) Nadler, E. B.; Rappoport, Z.; Arad, D.; Apeloig, Y. *J. Am. Chem. Soc.* **1987**, *109*, 7873 and references therein. (d) Hine, J.; Miles, D. E.; Zeigler, J. P. *J. Am. Chem. Soc.* **1983**, *105*, 4374. (e) Hine, J. *Acc. Chem. Res.* **1978**, *11*, 1. (f) Capon, B.; Siddhanta, A. K.; Zucco, C. *J. Org. Chem.* **1985**, *50*, 3580. (g) Krerge, A. J. *Acc. Chem. Res.* **1990**, *23*, 43.
(3) (a) House, H. O. *Modern Synthetic Reactions*, 2nd ed.; Benjamin: Menlo Park, 1972; pp 629-733, 459-461. (b) Berson, J. A.; Jones, M., Jr. *J. Am. Chem. Soc.* **1964**, *86*, 5019. (c) Conia, J. M.; LePerchec, P. *Synthesis* **1975**, 1. (d) Cookson, R. C.; Parsons, P. J. *J. Chem. Soc., Chem. Commun.* **1976**, 990.

0002-7863/91/1513-4530$02.50/0